Electronic Supplementary Information

Effect of Substrate Pre-treatment on Microstructure and Enhanced Electrochromic Properties of WO_3 Nanorod Arrays

Wenkuan Man[a], Hui Lu[b], Liangchen Ju[a], Feng Zheng[,c,d], Mei Zhang[a], and Min Guo[*,a]*

1. Figure S1 showed the XRD pattern of the as-prepared WNRAs grown TiO_2 seed layer annealed at 700 °C for 15 min under a hydrothermal process at 180 °C for 8 h. It can be seen that all the diffraction peaks could be well indexed to the standard diffraction pattern of hexagonal phase WO_3 (JCPDS 01-075-2187) except for the diffraction peaks indexed to the FTO substrate.

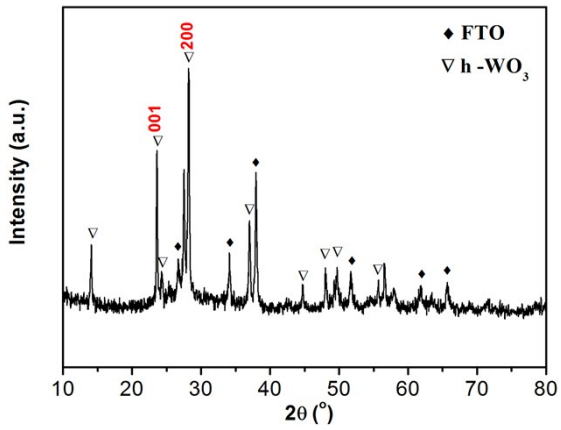

Figure S1 XRD pattern of the as-prepared WNRAs grown TiO_2 seed layer annealed at 700 °C for 15 min under a hydrothermal process at 180 °C for 8 h.

2. Figure S2 gave the SEM images of A_{Ti700} nanorod arrays before and after the CV

[a] *State Key Laboratory of Advanced Metallurgy, School of Metallurgical and Ecological Engineering, University of Science and Technology Beijing, Beijing 100083, P. R. China*

[b] *School of Materials Science and Engineering，Beifang University of Nationalities, Yinchuan Ningxia, 750021, P. R. China*

[c] *Materials Science and Engineering college, Shanghai University, Shanghai 200444,P. R. China*

[d] *Nano-science and Nano-technology Research Center, School of Materials Science and Engineering, Shanghai University, Shanghai 200444, P.R. China*

[*] *Corresponding author: Min Guo*; *Fax: +86 10 62334926*; Email: *guomin@ustb.edu.cn*

[*] *Corresponding author: Feng Zheng*; Tel.: +86(0)21 66137276; Email: *525zhengfeng@163.com*

test. It can be seen from Figure S2 that after cycling test, the shapes and growth orientation of the nanorods in A_{Ti700} didn't change, which meant the A_{Ti700} nanorod arrays had good structure and cycling stability.

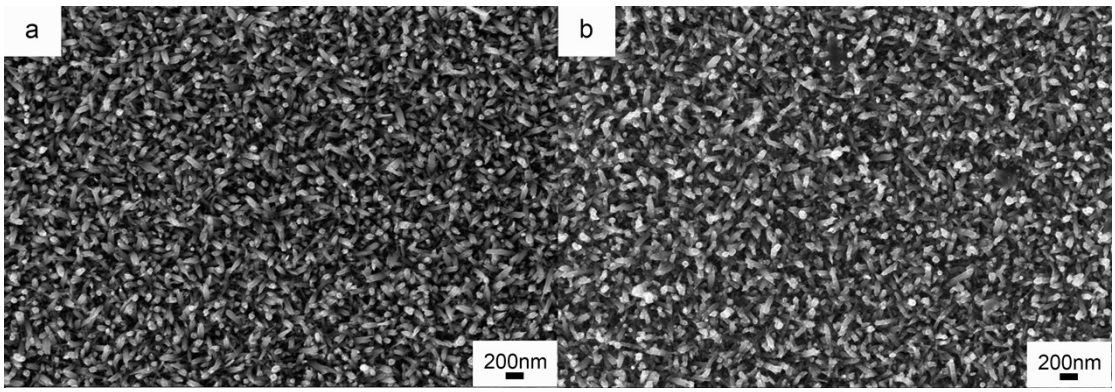

Figure S2 SEM images of A_{Ti700} nanorod arrays (a) before and (b) after CV test

3. Figure S3 illustrated the visible transmittance spectra of the as-prepared TiO_2 and WO_3 seed layers. It can be seen that the transmittance modulation of the TiO_2 seed layer was less than 3% ($Transmittance_{(at\ bleached\ state)}$ (85.7%)-$Transmittance_{(at\ colored\ state)}$ (82.8%)), while that of the WO_3 seed layer was larger than 24% (78.3%-53.8%) at the wavelength of 660 nm.

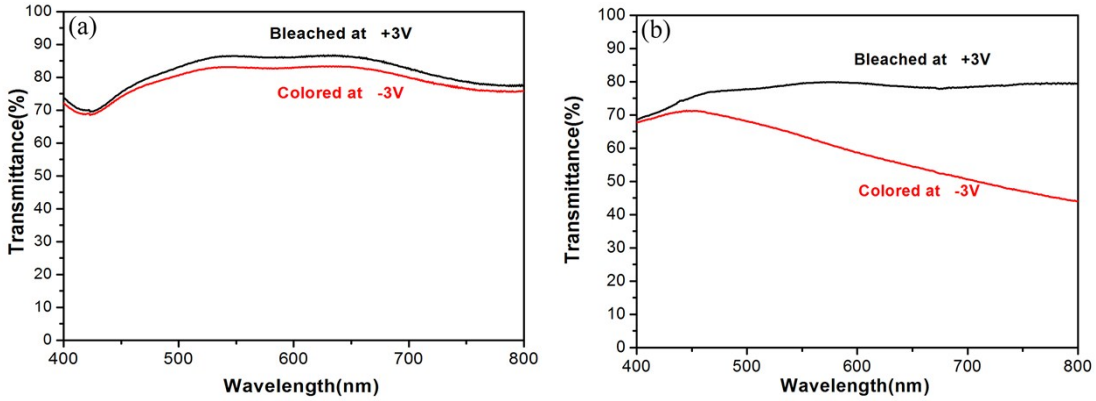

Figure S3 The visible transmittance spectra of (a) as-prepared TiO_2 seed layer annealed at 700 ^oC for 15 min and (b) WO_3 seed layer annealed at 500 ^oC for three times (10, 10, 30 min) at colored and bleached states when applied -3.0 V and +3.0 V for 100 s, respectively.

4. Figure S4 exhibited the plots of current density *vs*. time of the A_{Ti700} and A_W. As for A_{Ti700}, the sections of the current density *vs*. time plot at 100-200 s and 200-300 s corresponded to the coloring and bleaching process, respectively. The current densities could quickly reach their saturation after the voltage switching for both coloring and bleaching process, while, as for A_W, the current densities were slowly to get to their saturation, especially for the bleaching process. Compared with A_W, A_{Ti700} showed larger current densities and faster response after the voltage switching, indicating A_{Ti700} was easier for the intercalation/deintercalation of the Li^+ ions, thus major transmittance modulations for coloring and bleaching could be completed in shorter time. Moreover, A_{Ti700} showed smaller charge density for the accomplishment of the coloring and bleaching process than A_W, revealing that a serial of ΔOD values could be obtained in A_{Ti700} with smaller charge density.

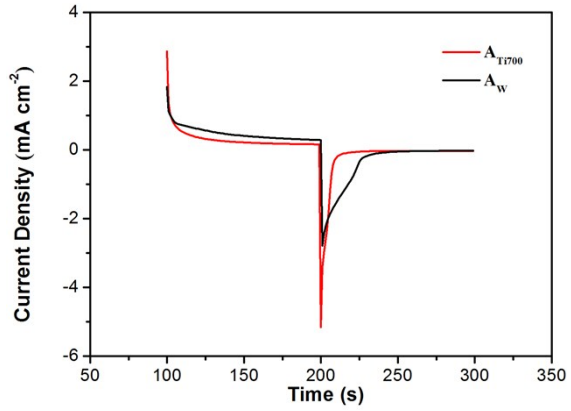

Figure S4 The plots of current density *vs*. time of the A_{Ti700} and A_W.

5. Figure S5 showed the SEM images of the TiO_2 seed layer annealed at different temperatures (550-700 ^oC) and WO_3 seed layer. It can be found that the grain sizes of the TiO_2 nanoparticles in the seed layers increased with increasing the annealing temperatures (Figure S5 (a)-(c)). According to the statistics from the corresponding SEM images, the average diameters of the TiO_2 nanoparticles were about 15.0, 25.0 and 35.0 nm, respectively, and the average grain size of the WO_3 seeds was about 37.5 nm.

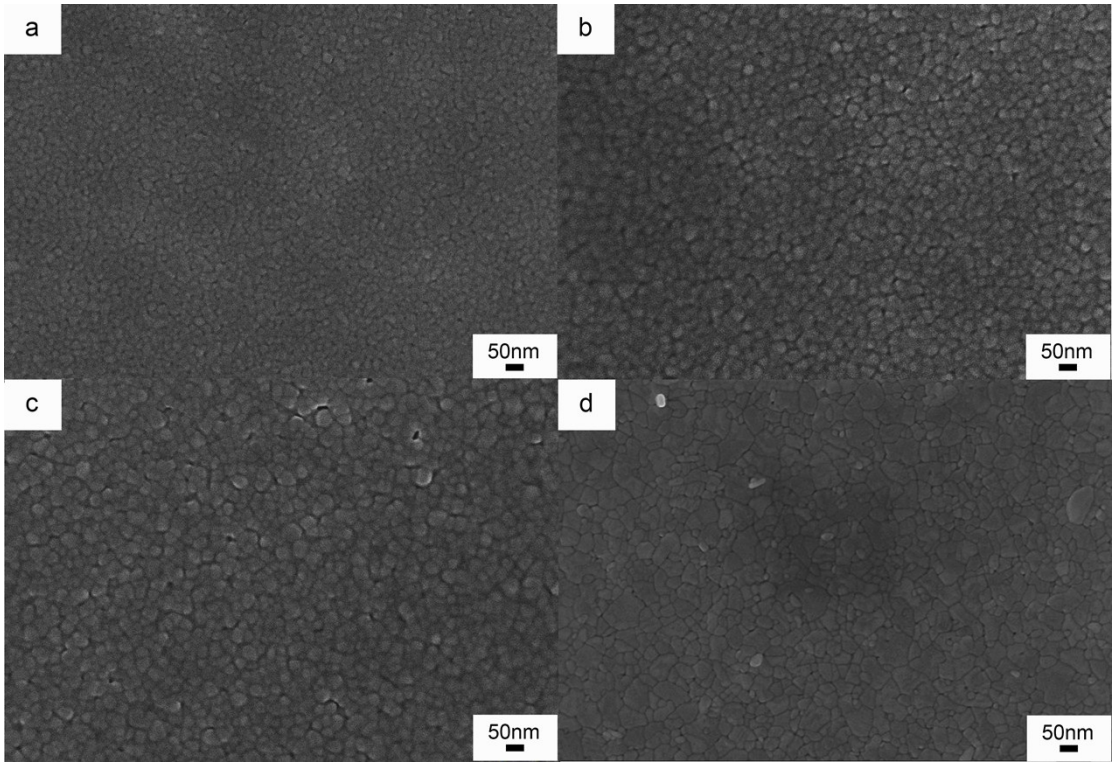

Figure S5 SEM images of the TiO_2 seed layers annealed at (a) 550 ^oC for 30 min, (b) 650 ^oC for 30 min and (c) 700 ^oC for 15 min and (d) WO_3 seed layer annealed at 500 ^oC.

6. The EIS of A_W and A_{Ti700} nanorod arrays were tested and the results were shown in Figure S6. The EIS tests were carried out by applying an AC voltage of 10 mV in the frequency range 100 kHz to 0.01 Hz at their bleached states. A Randles circuit model was used to fit data presented in the inset of Figure S6. The Randles circuit model comprised of series resistance (Rs) of the system (resulting from electrolyte/substrate resistance), Rct the charge transfer resistance (i.e. interfacial redox reaction resistance) connected in parallel with an electrical double layer capacitance (Cdl) at the electrolyte/electrode interface and finally the Warburg diffusion element (Zw) accounting from the ionic diffusion and charging of film. These parameters could be calculated by using ZSimpwin software (Table S1). From Table S1 it is known that the values of R_s, R_{ct} and Z_w of the A_{Ti700} were all smaller than those of A_W, further confirming the fast charge transfer which finally led to shorter switching time and higher coloration efficiency of the A_{Ti700}.

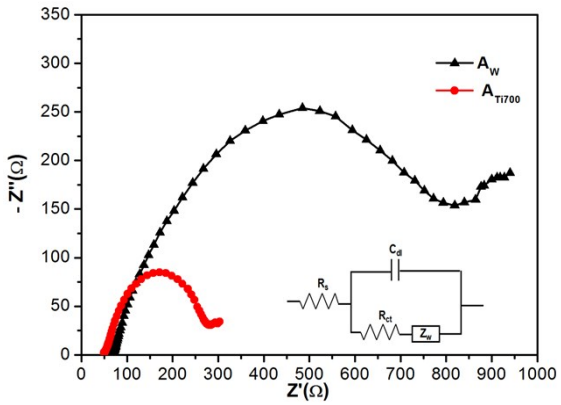

Figure S6 EIS of A_W (black) and A_{Ti700} (red)

Table S1 EIS parameters of A_{Ti700} and A_W obtained by fitting the data to Randles circuit.

	Rs (Ω)	Rct (Ω)	Zw (S $s^{1/2}cm^{-2}$)
A_W	77.2	487.7	0.04
A_{Ti700}	5.5	194.5	0.03